Troposphere Delay Model Error Analysis With Application to Vertical Protection Level Calculation

Yu-Fang Lai, Juan Blanch, Todd Walter
Stanford University

BIOGRAPHY

Yu-Fang Lai is a Ph.D. candidate at Stanford GPS Lab. He received Bachelor's degree in Aero/Astro from National Cheng-Kung University in 2020, and Master's degree in Aero/Astro from Stanford in 2022.
Juan Blanch is a senior research engineer at Stanford University. He is a graduate of Ecole Polytechnique in France, he holds an M.S. degree in electrical engineering and a Ph.D. degree in aeronautics and astronautics from Stanford University.
Todd Walter is a Professor at Stanford University and the faculty of Stanford GPS Lab. He received his B.S. degree in physics from Rensselaer Polytechnic Institute and his Ph.D. degree in 1993 from Stanford University.

ABSTRACT

In the L1 Satellite Based Augmentation System (SBAS) Minimum Operational Performance Standard (MOPS) the correlation of the tropospheric model correction error is treated as though it is uncorrelated from one satellite to another when computing the position error bound. This simplification has recently been called into question in Gallon et al. (2021). This paper examines the effect of neglecting this cross-satellite correlation on the protection level computation. We have found the lack of correlation terms to be conservative when generating the Horizontal Protection Level (HPL). However, there are cases where the Vertical Protection Level may be underestimated by neglecting this effect. For current operations where the Vertical Alert Limit (VAL) is 35 m and above, the effect is limited to about 2% of the MOPS VPL value. For smaller VALs, the effect can be much more significant, particularly is VALs below 10 m are considered. We recommend including the correlation term in bounding the tropospheric correction errors for the upcoming dual frequency SBAS MOPS.

We examine 10 years of tropospheric delay data collected and processed from hundreds of International GNSS Service (IGS) stations. 3 tropospheric models are used to analyze the residuals between IGS data and model predictions – University of New Brunswick 3 (UNB3), Global Pressure and Temperature 2 Wet (GPT2W) and Global Pressure and Temperature 3 (GPT3). Residuals are analyzed in terms of their probabilistic distribution in each IGS station. Stations are grouped and categorized by years and locations. It is found that residual distributions are most strongly dependent on latitude. In some infrequent cases where the IGS data appear to be anomalous and far from the model values, JPL data and actual weather record are used to evaluate and validate or reject the anomaly data. Finally, Gaussian pair-bounds are established in every station. An overall residual distribution is provided to account for the correction error caused by using the model. Finally, alternate forms for the SBAS VPL are provided to fully account for the cross satellite tropospheric model errors.

I. INTRODUCTION

The Wide Area Augmentation System (WAAS) is an SBAS program sponsored by Federal Aviation Administration (FAA), first developed in the late 1990s and declared operational in 2003. The objective is to increase the availability, accuracy and integrity of the Global Positioning System (GPS) without installing additional equipment at airports in the North America region. It collects measurements from ground reference stations and broadcasts correction signals through geostationary satellites. The MOPS (RTCA, 2006) regulate the operation and application of the correction signals so the definition of nominal error model and the protection level equations are essential to the integrity of the WAAS users. Currently, the L1 SBAS MOPS considers tropospheric delay errors as uncorrelated across satellites when calculating the protection level for position solution. It was acknowledged the tropospheric errors are almost always correlated since tropospheric delay on the user side primarily only differs by the line-of-sight elevation angle to the satellites. Although MOPS implemented the protection level as if the tropospheric error is always uncorrelated, this simplification has served well for standard requirement when the AL is above 35 m for standard nominal error model. However, as demonstrated in this paper, this assumption might not always valid for VAL is below 10 m.

This paper focus on VPL equation on L1 single frequency in the current SBAS MOPS, and Juan Blanch (2023) has the tropospheric error analysis on dual frequency and Advanced Receiver Autonomous Integrity Monitoring (ARAIM).

We inspect three tropospheric models, UNB3 (Collins and Langley, 1997), GPT2W (Böhm et al., 2015) and GPT3 (Landskron and Böhm, 2018), with 10 years of tropospheric delay data collected and processed by IGS to determine the paired-bounds statistics that bounds model error distribution over the past 10 years. Without changing the nominal error model, we propose an alternate form of VPL equation that can be easily adapted to the system which includes the effect of correlation and modelling error of UNB3, the tropospheric model MOPS adopted. EUROCAE (2023) identifies that the simplification of tropospheric correlation between vertical position error and VPL could lead to error in VPL prediction, and McGraw (2012) points out the simplification need to be taken into account for tropospheric error bounding for improved performance.

In Gallon et al. (2021), the tropospheric residual is first defined as the value difference between model prediction and IGS estimation. Both UNB3 and GPT2W are evaluated against a Gaussian CDF bound over a year of data across 100 IGS stations chosen worldwide. It is shown UNB3 model has larger bias and standard deviation than GPT2W.

DeCleene (2000) proposed that the positioning error can be bounded if the underlying pseudorange error Probability Density Function (PDF) is symmetric and unimodal, and if its CDF is bounded by a Gaussian CDF, then the position error is bounded as well. Rife et al. (2006) relaxes the assumptions of symmetric and unimodal PDF via constructing a pair of Gaussian bounding region that the error CDF is bounded as long as inside the region. The weakness of pair-bounding is it requires the empirical error distribution to be strictly bounded and it turns out to be an impossible requirement for empirical probability distribution since it would fail at the head and at the tail of the CDF, where Gaussian distribution is unbounded. It implies any paired-bound to empirical probability distribution is an approximation. The two-step bounding (Blanch et al., 2018) resolve this issue by first determining an intermediate symmetric and unimodal Gaussian paired-bound, then relaxing the bounding with excess mass parameter. The resulting overbounding provides much smaller bias.

The rest of the paper is structure as follows, Sec.II describes the concept of tropospheric delay and the general structures for tropospheric models. Sec.III introduces the data set used in this paper and the definition of tropospheric residual. Sec.IV analyzes the UNB3 residual with different grouping criteria and Quantile-Qauntile plot (QQ-plot) representation. Sec.V explains the Ad-hoc algorithm for computing tight paired-bound for residual distribution. Sec.VI demonstrates and discuss the paired-bound for the past 10 years of residuals. Finally, Sec.VII proposes an alternate VPL equation accounting correlation and utilizing paired-bounding parameters.

II. TROPOSPHERE DELAY MODELS: UNB3, GPT2W AND GPT3

The troposphere is the lowest layer of atmosphere above the earth. It is the region where all the weather events happens, such as rain and hurricanes. One important aspect of troposphere is the medium consisted is non-dispersive, meaning the induced time delay of radio waves (i.e. the GPS signal) when passing through the troposphere are equally affected across frequency domains. Therefore, applying dual frequency signal cannot eliminate delay in troposphere as the delay in ionosphere, which has dispersive medium. Mathematical models are established in order to estimate and reduce the effect of tropospheric delay on GPS signals.

Two main components in the troposphere cause delay to GPS signal, the hydrostatic delay and the wet delay. The first part, hydrostatic delay, or dry delay, is the delay induced by the dry gases in troposphere (78% N_2, 21% O_2...). The dry part of troposphere typically cause 2.3 $\sim$ 2.6 m of delay to the signal in zenith direction, and up to 20 m as the mapping function at 5 degrees is around. The second part, wet delay, is the delay caused by water vapor and condensed water. This part of the delay varies from 0 $\sim$ 40 cm in zenith direction, and 0 $\sim$ 2 m in lower elevation angle. The dry component is considered to be stable due to the fact the dry gases vary predictably through years and locations. On the other hand, the wet component is highly stochastic in the sense that water vapor and condensed water can change from 0 to 100% humidity in a very short period of time, making it difficult to model. Thus, the wet delay behavior is relatively unpredictable compared to the dry delay and is the main source of randomness when estimating tropospheric delay. Despite that dry delay is several times greater than wet delay in most cases, the wet delay predominantly contribute to the uncertainties of tropospheric delay estimation when applying tropospheric models.

The Mapping function is another important part of tropospheric models. It maps dry and wet delay components from zenith direction to line-of-sight direction. Since GPS signals travel farther in the troposphere if the satellite is at low elevation angle, the signals stay longer inside troposphere and introduce more delay to itself. As a result, the lower the elevation angle, the greater the mapping function in order to account for the additional delay. Because satellites are all at different locations and therefore elevation angle, however the tropospheric delay is all concentrated to a small region around receiver, resulting in strong correlation. This is the relation simplified in the current VPL equation.

The tropospheric delay models examined in this paper (UNB3, GPT2W and GPT3) have similar structure. First, the models predict the dry and wet delay components in zenith direction, then compute mapping function for both components in terms of the satellite locations, then apply mapping functions to the zenith values, eventually combine them to obtain the slant total delay (STD). UNB3 (Collins and Langley, 1997) model is adopted by SBAS MOPS as their tropospheric delay model for

correction broadcast. It relies on a simple 15° latitude-wise lookup table for estimating parameters such as barometric pressure, temperature and water vapour pressure. The resulting parameters are then applied to an improved Sasstamoinen model (Davis et al., 1985) to obtain dry and wet delay in zenith direction, and Black and Eisner Mapping function (Black and Eisner, 1984) for the mapping function values. GPT2W (Böhm et al., 2015) and GPT3 (Landskron and Böhm, 2018) were developed for the purpose of geodesy application, and were designed for accuracy. They use $1^\circ \times 1^\circ$ grid map built from 10 years of empirical data to estimate necessary parameters such as pressure, temperature and mapping factors, and more complicated mapping functions. GPT3 is the successor of GPT2W. GPT series are typically more precise than UNB3 but require more computations and larger storage space for the table.

III. THE DATASET AND RESIDUALS

International GNSS Service, IGS (2022), has around 400 GNSS receiver stations world-wide and provide free access to varies GNSS products. The number of stations available may vary form days to days due to new stations introduced, old stations retired or station maintenance. In this paper, We include every station available from year 2012 to 2021 to verify the effectiveness of the Gaussian paired-bound we establish. The tropospheric Zenith Path Delay (ZPD), or Zenith Total Delay (ZTD), is the GNSS product we are examining in this paper. ZTD is the summation result of both dry and wet delay in zenith direction from the corresponding stations, and is treated as baseline in the analysis of tropospheric models.

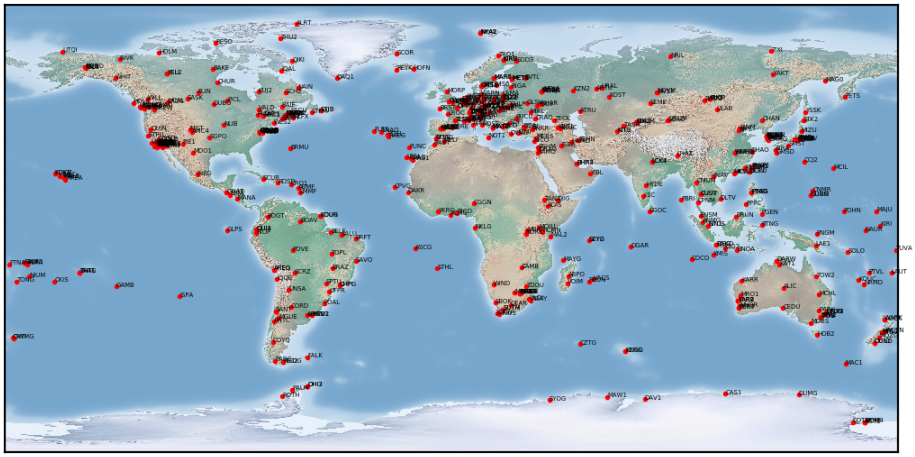

Figure 1: IGS Map and stations. IGS (2022)

We define tropospheric zenith residuals as difference between ZTD from IGS and ZTD predicted by models:

$$R_{model} = ZTD_{Model} - ZTD_{IGS}$$

where R_{model} is the residual of the model, ZTD_{Model} is the ZTD estimated from the model, and ZTD_{IGS} is the ZTD data from IGS.

In some infrequent cases, we observe that the magnitude of the residuals exceed 28 cm, the maximum deviation of UNB3 model regulated in MOPS. It is sometimes due to a reset of the filter, which may take time to converge to the true value from an initial guess, or sometimes due to a losing track of the signals, unusual weather conditions such as hurricane, extremely dry or wet day, monsoon season, or lack of maintenance to the receiver itself. We review the weather report on those days having abnormal residual values, in particular, the days with residuals magnitude greater than 28 cm. Since the ZTD value is expected to be within certain reasonable range. For example, even in the most extreme cases, where temperature is 100° Celsius, pressure is at extreme limit, humidity is 0% or 100% saturated, the possible tropospheric delay value can be observed on earth is bounded. Without loss of integrity to the tropospheric delay value, we review weather reports on those anomalous days, and exclude them if the weather reports show nothing abnormal.

In addition to IGS data, Jet Propulsion Laboratory (JPL) produce similar tropospheric delay product using GipsyX (Bertiger et al., 2020), in their Making Earth System Data Records for Use in Research Environments (MEaSUREs) program (Vollmer et al., 2011). While the number of stations (around 1800 stations) JPL process are significantly greater than IGS, the majority of the stations are located in North America region, so JPL data are better choice for evaluating North America region but the global analysis is better using IGS data. Therefore, JPL data are served as supplemental verification to IGS data given they only

share 40s stations worldwide, limiting the scope of cross-validation on IGS stations.

IV. RESIDUALS ANALYSIS

1. The Grouping Criteria

IGS stations are grouped every five stations and every 5° latitude, meaning each group has at most 5 stations and across at most 5 degree in latitude.The purpose is to look for a dependency on Latitude and the reason for grouping station in this way is to retain a minimum number of stations per group and location without having excess number of stations concentrated in one group, because most IGS stations are located in $30^\circ N \sim 50^\circ N$.

2. Quantile-Quantile Plot

Quantile-Quantile Plot (QQ-plot) is a way of representing data distribution in terms of the quantile of data and quantile of a reference distribution. If the data present on the QQ-plot is a straight line with slope of one, the data is distributed the same as the reference distribution. A common choice for reference distribution is standard normal distribution.

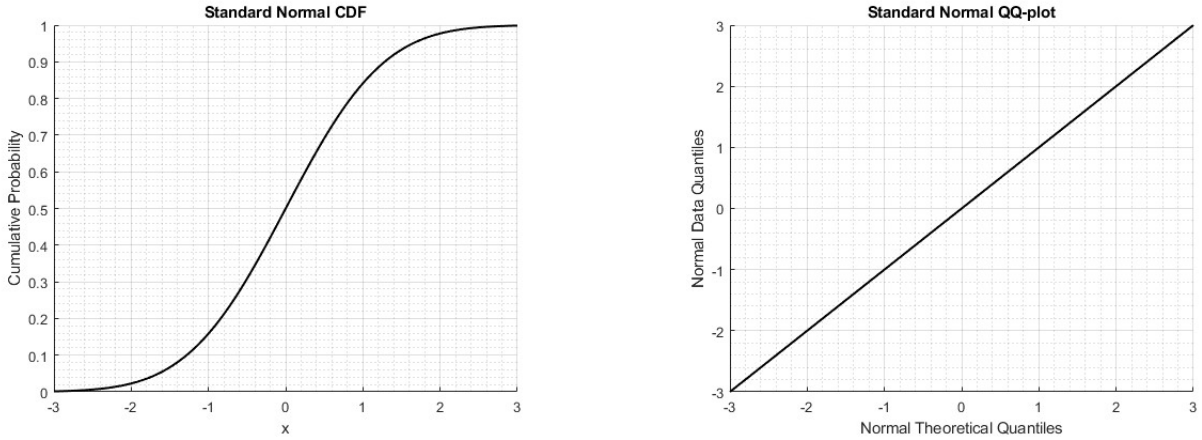

(a) Normal Empirical CDF

(b) QQ-plot

Figure 2: Normal CDF and QQ-plot

Fig.2a is a conventional representation of CDF, having a S-curve as we often see. Fig.2b is an example of QQ-plot. For standard normal quantiles, the slope of the line represents standard deviation and displacement in vertical direction at zero quantile represents mean. QQ-plot allows more convenient way of determining paired-bound condition for empirical data. The Gaussian paired-bound are a pair of straight lines in QQ-plot and the bounding region becomes a simple interval defined by two straight lines. In the rest of the paper, we treat QQ-plot as our default representation of tropospheric residual.

3. Residual Distribution

The residual distribution vary little throughout years, so in this section we would examine the most recent year, the data in 2021.

a) UNB3

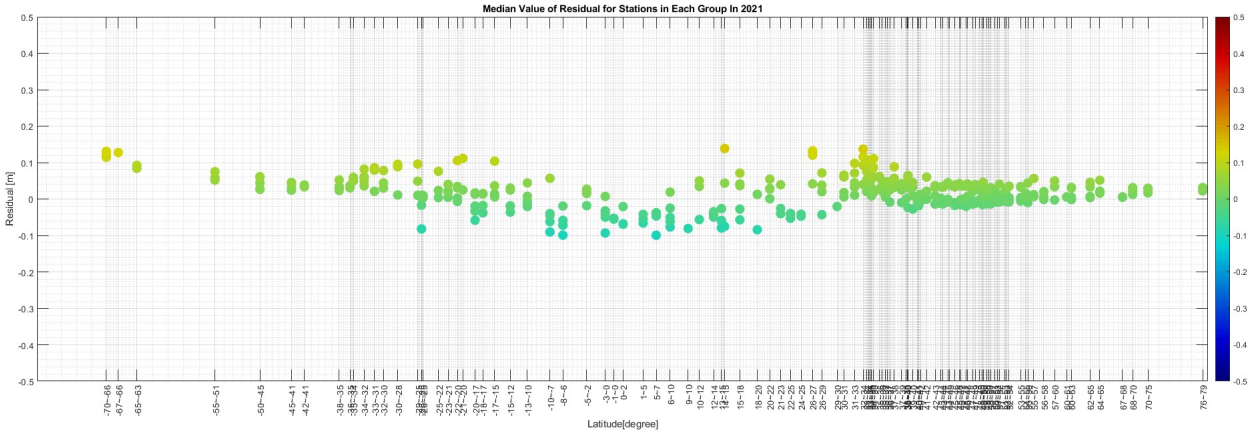

Figure 3: Median residuals of UNB3 model in 2021.

Fig.3 shows the median of UNB3 at all IGS stations in 2021, which is the residual with half cumulative probability. The medians are grouped in latitude and are displayed in scale with the actual latitude. The medians are densely compact in latitude $30° \sim 50°$, because the majority of IGS stations are located in these latitudes. This region is also where the most of the data used to create the UNB3 model was taken from, so we can see UNB3 performs relatively stable in this region and above, with the medians generally smaller than 10 cm. There are fewer stations below $30°$ south, and the medians are less stable and less accurate as in southern hemisphere, with many stations having medians less than 10 cm and greater than -10 cm. There are only 25 stations located in $-40° \sim -70°$, the medians rise as the latitude become lower, and are all greater than 10 cm for stations below $-65°$, which are stations in Antarctica. The reason for this is UNB3 appears to have simplified the model by assuming the symmetry to weather environments in northern and southern hemisphere, in the sense that the temperature and pressure conditions are similar in the same latitude region for northern and southern hemisphere. This is a reasonable approximation as the medians are in general distributed symmetric with respect to $0°$, the equator. However, the symmetry does not hold for latitude below $-65°$ where the Antarctica continent located. Despite the symmetric approximation, all stations are having medians less than 17 cm and greater than -10 cm. The median values of stations are an essential factor to the paired-bound of the residual distributions as they limit the minimal value of bounding bias.

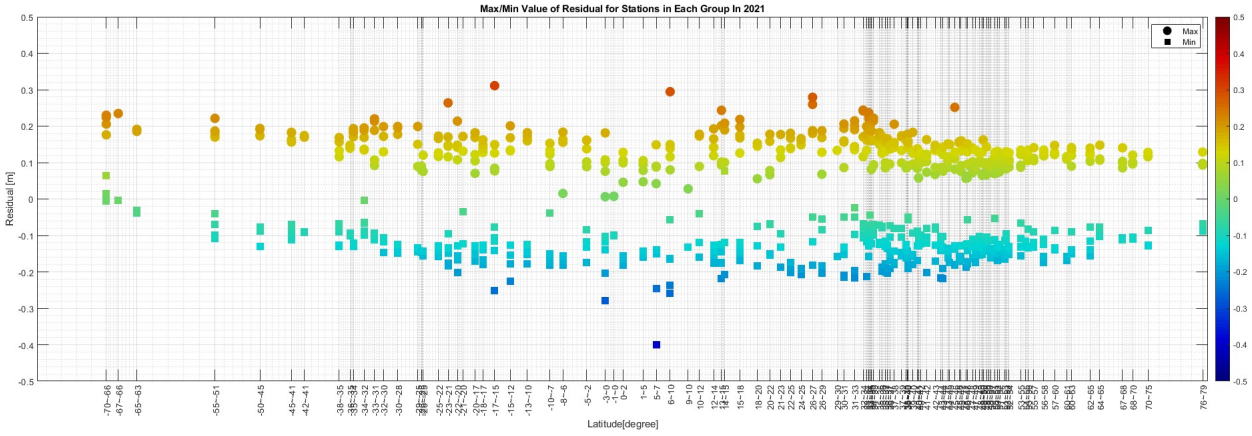

Figure 4: Maximal and Minimal residuals of UNB3 model in 2021.

Fig.4 shows the maximal and minimal residuals for all stations in 2021, where the circle represents maximum and the square represents minimum. The extremum indicate the worst estimation of UNB3 in the stations, and how wide-spread the distribution.

Here we can observe there exist multiple stations having maximal residual as much as 30 cm, and minimal residual down to -40 cm, which are unusually large residual error magnitudes. The definitive parameters to tropospheric delay include pressure, temperature, humidity and altitude. For one location to have -40 cm residual, it demands extreme weather condition such as low pressure, low humidity and high altitude, and there are limitations on how low a tropospheric delay can be. For instance the humidity cannot go below complete unsaturation or above complete saturation, so if a station reports unusual low or high residuals, there must be an extreme weather event happening nearby the receiver, such as hurricane, tornado, extremely high or low temperature, pressure etc. Consequently, we evaluate the weather record on the days the abnormal residual is computed, and exclude the data points from the computation of the residual distribution if the weather record reports regular result. The station with -40 cm residual in 2021 is ACRG, a station located in Accra, Gahna, where the receiver is 83 m above sea level. The weather record shows fairly moderate weather condition on the day having -40 residual, April 20th2021. The temperature ranged from $79°\text{F} \sim 93°\text{F}$, humidity from $20\% \sim 75\%$, pressure from 29.58 inch ~ 31.53 inch, and no precipitation. From this point of view, the day with -40 cm residual is no different from the days before and after, when the residuals magnitude were well within 28 cm. Thus, we conclude the -40 cm residual do not reflect the true residual and should be removed from the data set. The cause to this failure has not been identified but might be due to the filter reset, lost track of signal or device glitch.

Without loss of integrity, we evaluate weather records on the days the stations with residual magnitude greater than 28 cm, and exclude data points if it does not record usual temperature, humidity and pressure. For some stations where JPL data are available, the JPL data are used to cross-validate the IGS data along with weather record. 28 cm is the number we picked and is not the basis for data rejection. The basis for rejection is when the weather condition were not extreme, the filter behavior is unusual, and it does not match a cross-comparison when available. Other number such as 25 or 22 cm can be easily adopted to subsequent analysis.

In short, if the residual magnitude is greater than 28 cm, the data will be evaluated and excluded if the corresponding weather record is normal and is not consistent with the day before and after, otherwise they will not be excluded.

There are three days of data contain residual magnitude greater than 28 cm in 2021 for UNB3, STHL on Jan. 26th, ACRG on April 20th, and SGOC on April 22th. The weather record suggest all three of them should be excluded from the computation of residual distribution.

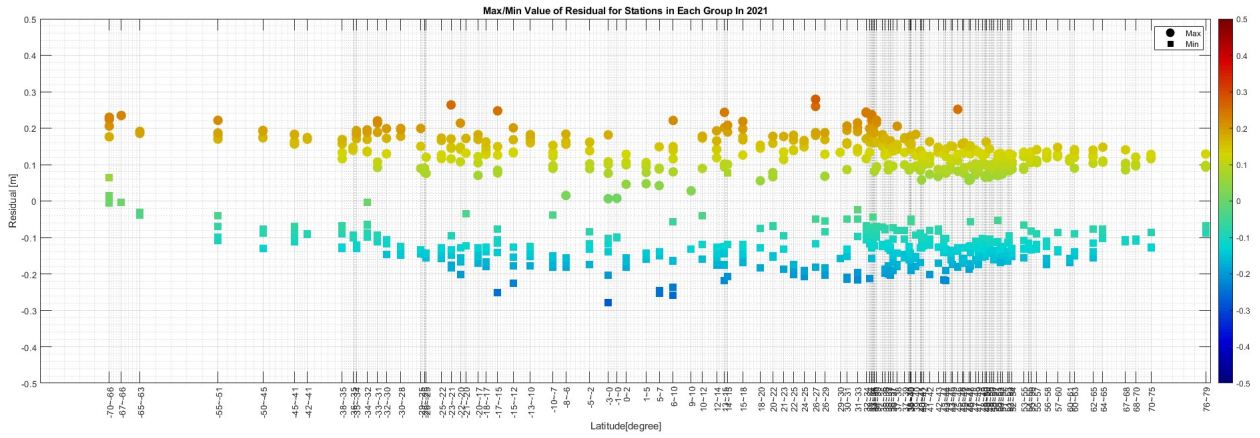

Figure 5: Maximal and Minimal residuals of UNB3 model in 2021 after removal of data.

Fig.5 is the maximal and minimal residuals of all IGS stations in 2021 after data exclusion. As Fig.3, the extreme residuals are symmetric about the equator with the stations in Antarctica biased by about 10 cm comparing to stations in the north. The stations in northern hemisphere are concentrated and relatively stable, with only few stations having residual magnitude greater than 20 cm. The extrema affect the bounding in head and tail regions, which may amplify the bound since it is necessary to enclose residual distribution on the entire residual space, and few extreme cases could enlarge the bias or variance of the bound so as to completely include the residual.

b) GPT2W and GPT3

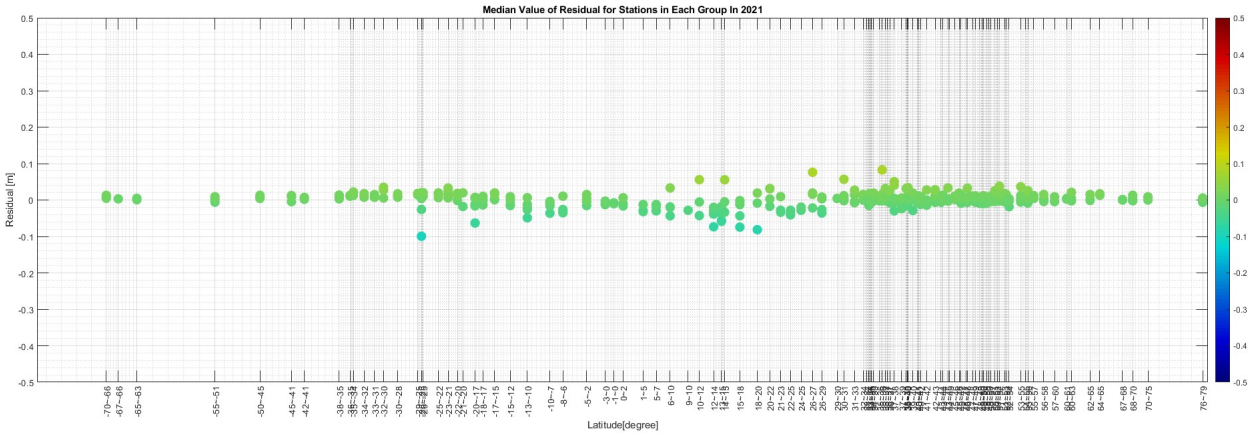

Figure 6: Median residuals of GPT2W model in 2021.

Fig.6 is the median residual of GPT2W in 2021. The medians are more consistent and closer to zero compared to UNB3 in Fig.3. Since GPT2W rely on $1° \times 1°$ empirical grid point data for parameters such as temperature and pressure, there is no symmetric error issue for stations in Antarctica region, and the median magnitude are all within 10 cm. This property implies the minimal bias for bounding GPT2W residuals are consistent throughout different latitude, and the resulting overall bound is less conservative to be used in different location.

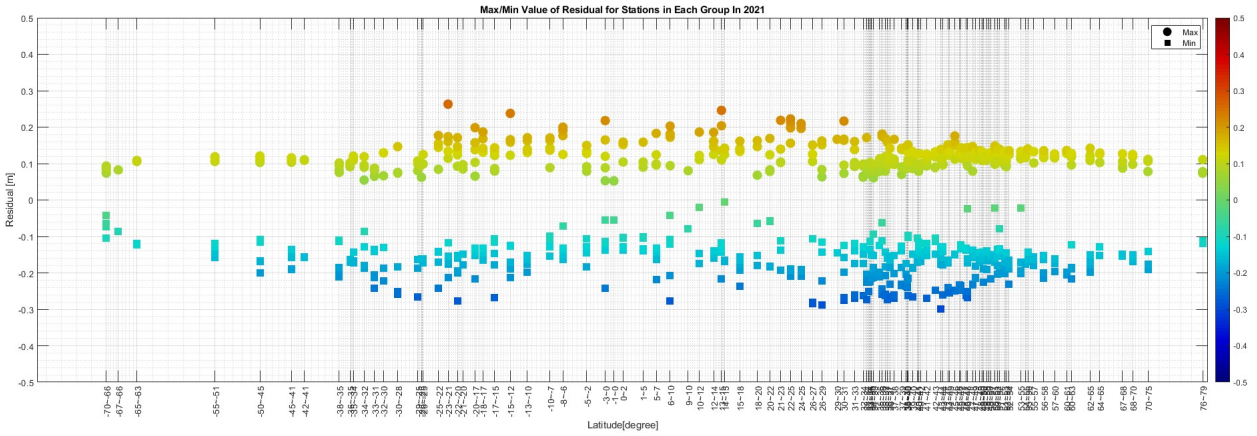

Figure 7: Maximal and Minimal residuals of GPT2W model in 2021.

Fig.7 is the maximal and minimal residuals for GPT2W in 2021 after excluding few data points. Note there are some stations with minimal residual less than 28 cm. The weather record have been evaluated and the data evolved continuously before and after, so we conclude that the tropospheric delay estimation from IGS station on those days were reflecting the real situation and should not be excluded from the computation of distribution. The maximal residual from GPT2W are more stable and concentrated than the minimal residual. The latter is more scattered and distributed in a way similar to UNB3, which could potentially result in greater paired-bound variance in order to bound the tail distribution. As for Antarctica region, the extrema distribute less biased as median.

GPT3 model is the successor of GPT2W with improved mapping function and empirical grid points for interpolation. However, the resulting residual distribution is nearly identical to GPT2W so the median and extrema residual distribution are omitted here for simplicity.

For data in $2012 \sim 2020$, the residual is not shown here for the same reason.

From the perspective of median and extrema residuals, GPT models possess less biased estimation of tropospheric delay, with all of them under 10 cm of residual magnitude, and have no symmetric biased issue in southern hemisphere, and the maximal residual is more consistent and align with IGS data, but the minimal residual resemble the distribution of UNB3. In contrast, the median and extrema of UNB3 are more biased and less concentrated. However, UNB3 can compute tropospheric delay much faster and need less memory storage whilst GPT models require much larger computational resources.

V. PAIRED-GAUSSIAN BOUNDING

The bounding of a distribution is achieved such that the probability of any interval of a data CDF is lower than the distribution of an upper bound and greater than an lower bound. In the case of tropospheric residual distribution, the upper and lower bound imply the worst case scenario for the uncertainties of tropospheric model prediction, hence the bounding to the residuals provides a conservative correction for VPL.

The paired-bounding theorem relies on Gaussian distribution as the distribution of the upper and lower bound. The issue with single Gaussian bound is if the distribution has different median, the bound would inevitably fail at the median. As a result, an additional parameter, bias, is added to ensure the upper and lower bounds are everywhere overbounded to the distribution within the bias region.

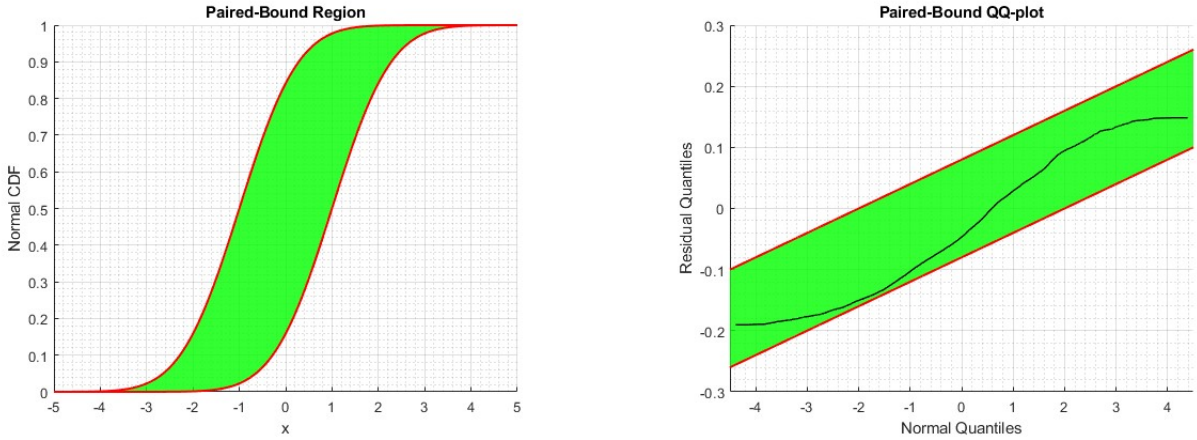

(a) Gaussian Bounding with Bias

(b) Paired-Bound QQ-Plot

Figure 8: Gaussian Paired-Bound

Fig.8a is the paired-Gaussian bound. The paired-bounding theorem define a wider region of bounding envelope. Any distribution falls inside the envelop is considered bounded and the paired-bound can be described with two parameters, σ and β, where σ is the standard deviation of Gaussian distribution, and β is the bias of the bound, it is the displacement of upper and lower bound from zero quantile. Note that while having different σ for the the paired-bounds is possible, here we let the both sides of the bound share same σ, so the bound must be symmetric. The advantage of defining bound in this way is that the entire pair-bounds can be determined with two parameters, σ and β. Fig.8b is the QQ-plot representation of the paired-bound. It enables simpler logic for developing the Ad-hoc Algorithm since the boundedness is now defined by two straight lines.

One potential issue with paired-bound is when bounding multiple distribution as we do for tropospheric residuals. From the perspective of protection level, a paired-bound with larger bias and standard deviation is guaranteed to overbound a paired-bound with smaller parameters. However, from the paired-bound perspective, a distribution might not be bounded with larger parameters. For example, if the standard deviation of the paired-bound in Fig.8b is increased, the bounding for the distribution will fail, but the protection level is still valid.

To ensure the nominal error model conservatively bound the residual distribution, the Ad-hoc Algorithm calculates suitable pairs of β and σ on each residual distribution, and retain the maximal β and σ for groups of residuals.

1. Ad-hoc Algorithm

The Ad-hoc algorithm numerically searches for the upper and lower bound to the QQ-plot of stations in a group. We define the condition for distributions to be considered bounded as:

$$B_{lo}(\beta,\sigma) \leq Q_i(X) \leq B_{up}(\beta,\sigma)\ \forall i \in \text{Station}\{1,...,N\} \tag{1}$$

where Q_i is the QQ-plot of station i in the group, X is random variable representing tropospheric delay residuals, β is bias and σ is standard deviation to the paired-bound B.

We ignore the first and last probability points in the distribution and any bound satisfies Eq.(1) is a permissible bound, and there are infinite combinations of β and σ. In order to narrow down the bounding solutions, we add three extra criteria and formulate the process of searching for the bound as optimization problems:

a) Minimum Bias

$$\begin{aligned} &\min_{\beta,\sigma}\ \beta \\ &\text{s.t. } B(-\beta,\sigma) \leq Q_i(X) \leq B(\beta,\sigma)\ \forall i \in \text{Station}\{1,...,N\} \end{aligned} \tag{2}$$

where we minimize bias by selecting a pair of bias and standard deviation.

b) Constant β

$$\begin{aligned} &\min_{\sigma}\ \sigma \\ &\text{s.t. } B(-\beta,\sigma) \leq Q_i(X) \leq B(\beta,\sigma)\ \forall i \in \text{Station}\{1,...,N\} \\ &\beta = \beta_0 \end{aligned} \tag{3}$$

where we minimize σ with a constant bias.

c) Constant σ

$$\begin{aligned} &\min_{\beta}\ \beta \\ &\text{s.t. } B(-\beta,\sigma) \leq Q_i(X) \leq B(\beta,\sigma)\ \forall i \in \text{Station}\{1,...,N\} \\ &\sigma = \sigma_0 \end{aligned} \tag{4}$$

where we minimize β with a constant standard deviation.

The reason for calling this Ad-hoc algorithm is the solution to the above optimization problems is computed through a series of numerical operations that are specifically designed and only applicable to the search of paired-bound for tropospheric QQ-plot presented here. The algorithm is as follow:

Algorithm 1 Determine if residuals are inside Paired-Bound B

```
procedure INSIDE(Q,β,σ)
    For Q_i in Q
        IF B(−β,σ) ≥ Q_i OR B(β,σ) ≤ Q_i
            return False
    return True
```

Algorithm 2 Find minimal bias given constant standard deviation

procedure FINDBIAS($\boldsymbol{Q}$,β_{init},σ,ϵ)
  Parameters
  $\beta_{up} \leftarrow \beta_{init}$
  $\beta_{lo} \leftarrow \beta_{init}$
  $\beta_{return} \leftarrow \phi$
  $\gamma \in (1.1, 2)$
  For Q_i **in** $\boldsymbol{Q}$
    IF INSIDE($Q_i, \beta_{init}, \sigma$)
      UNTIL INSIDE(Q_i, β_{lo}, σ) **IS** FALSE **DO** $\beta_{lo} \leftarrow \beta_{lo}/\gamma$
    ELSE
      UNTIL INSIDE(Q_i, β_{up}, σ) **IS** FALSE **DO** $\beta_{up} \leftarrow \beta_{up} \cdot \gamma$
    WHILE $\|\beta_{up} - \beta_{lo}\| \geq \epsilon$
      $\beta_{mid} \leftarrow \frac{\beta_{lo}+\beta_{up}}{2}$
      IF INSIDE(Q_i, β_{mid}, σ)
        $\beta_{up} \leftarrow \beta_{mid}$
      ELSE
        $\beta_{lo} \leftarrow \beta_{mid}$
    $\beta_{return} \leftarrow$MAX($\beta_{return}$,$\beta_{up}$)
  return β_{return}

Algorithm 3 Find minimal standard deviation given constant bias

procedure FINDSIGMA($\boldsymbol{Q}$,β,σ_{init},ϵ)
  Parameters
  $\sigma_{up} \leftarrow \sigma_{init}$
  $\sigma_{lo} \leftarrow \sigma_{init}$
  $\sigma_{return} \leftarrow \phi$
  $\gamma \in (1.1, 2)$
  For Q_i **in** $\boldsymbol{Q}$
    UNTIL INSIDE(Q_i, σ_{up}, σ) **IS** True **DO** $\sigma_{up} \leftarrow \sigma_{up}/\gamma$
    $\sigma_{lo} \leftarrow \sigma_{up}$
    UNTIL INSIDE(Q_i, σ_{lo}, σ) **IS** FALSE **DO** $\sigma_{lo} \leftarrow \sigma_{lo} \cdot \gamma$
    WHILE $\|\sigma_{up} - \sigma_{lo}\| \geq \epsilon$
      $\sigma_{mid} \leftarrow \frac{\sigma_{lo}+\sigma_{up}}{2}$
      IF INSIDE(Q_i, β, σ_{mid})
        $\sigma_{up} \leftarrow \sigma_{mid}$
      ELSE
        $\sigma_{lo} \leftarrow \sigma_{mid}$
    $\sigma_{return} \leftarrow$MAX($\sigma_{return}$,$\sigma_{up}$)
  return σ_{return}

Algorithm 4 Find minimal bias

procedure FINDMINBIAS($\boldsymbol{Q}$,β_{init}, σ_{init},ϵ,N)
  Parameters
  $\sigma_{return} \leftarrow \phi$
  $\beta_{return} \leftarrow \phi$
  $\boldsymbol{\sigma_{sample}} \leftarrow \phi$
  $\boldsymbol{\beta_{sample}} \leftarrow \phi$
  For Q_i **in** $\boldsymbol{Q}$
    $\boldsymbol{\sigma_{sample}} \leftarrow$ linspace(0,σ_{init},N) ▷ linspace creates a equally spaced vector ranged from 0 to σ_{init} with size N
    WHILE$\|MAX(\boldsymbol{\sigma_{sample}}) - MIN(\boldsymbol{\sigma_{sample}})\| \geq \epsilon$
      For σ_i **in** $\boldsymbol{\sigma_{sample}}$
        $\beta_i \leftarrow$FINDBIAS($Q_i, \beta_{init}, \sigma_i$)
      $I \leftarrow argmin(\boldsymbol{\beta_{sample}})$
      IF $I \leq N/2$
        $\boldsymbol{\sigma_{sample}} \leftarrow$linspace(MIN($\boldsymbol{\sigma_{sample}}$),$\boldsymbol{\sigma_{sample}}[ceil(N/2)]$,N)
      ELSE
        $\boldsymbol{\sigma_{sample}} \leftarrow$linspace($\boldsymbol{\sigma_{sample}}[floor(N/2)]$,MAX($\boldsymbol{\sigma_{sample}}$),N)
      $\beta_{min} \leftarrow \boldsymbol{\beta_{sample}}[I]$
      $\sigma_{min} \leftarrow \boldsymbol{\sigma_{sample}}[I]$
    $\beta_{return} \leftarrow MAX(\beta_{return}, \beta_{min})$
    $\sigma_{return} \leftarrow MAX(\sigma_{return}, \sigma_{min})$
  return (β_{return},σ_{return})

Algorithm 5 Search Paired-Bound

procedure SEARCHPAIREDBOUND($\boldsymbol{Q}$, α, β, σ, ϵ, N)
  Parameters
  $\beta_{return} \leftarrow \beta$
  $\sigma_{return} \leftarrow \sigma$
  SWITCH α
    Minimal Bias:
      (β_{return},σ_{return})$\leftarrow$FINDMINBIAS($\boldsymbol{Q}$,β, σ,ϵ,N)
    Constant Bias:
      $\sigma_{return} \leftarrow$FINDSIGMA($\boldsymbol{Q}$,$\beta$,$\sigma$,$\epsilon$)
    Constant Sigma:
      $\beta_{return} \leftarrow$FINDBIAS($\boldsymbol{Q}$,$\beta$,$\sigma$,$\epsilon$)
  return ($\beta_{return}, \sigma_{return}$)

Algorithm.(2) computes paired-bound bias given a constant standard deviation. $\boldsymbol{Q}$ are the residuals in QQ-plot, β_{init} is the initial value for bias, σ is the constant standard deviation, and ϵ is the tolerance for iterations. The algorithm first searches the upper and lower bound of the bias. The upper bound bias is guaranteed to bound the residual, and the lower bound is to not. A binary search method is used to narrow down the upper and lower bound bias until the difference is less then the tolerance. The searching process is performed to each station residuals, and the maximal bias is returned. Similarly, Algorithm.(3) minimizes standard deviation that bounds the residuals given a constant bias. β is constant bias specified by the user, and σ_{init} is the initial standard deviation for iterations. The σ_{init} should be sufficiently large such that the residual is not bounded initially. The subsequent line search would determine upper bound of σ by reducing σ_{init}. Once a feasible upper bound is found, the line search continues to reduce σ until the residual is not bounded to obtain the lower bound σ. With upper and lower bound σ, we apply binary search to minimize σ. Finally, Algorithm.(4) search for paired-bound that has minimal bias. To overcome the difficulties of multivariate minimization, we first create a vector of standard deviation equally spaced from 0 to σ_{init} with N elements, called $\boldsymbol{\sigma_{sample}}$, then find samples of minimal bias,$\boldsymbol{\beta_{sample}}$, associated with $\boldsymbol{\sigma_{sample}}$ via Algorithm.(2), and binary search the region contains lowest value of bias in $\boldsymbol{\beta_{sample}}$. The process is repeated until $\boldsymbol{\sigma_{sample}}$ converge, and the maximal β and σ are reported from each residual computation. This multivariate minimization process assumes the minimal σ to minimal β relations to be unimodal for all residual distribution. The computation result shows it is a sufficient assumption and can yield minimal bias on all IGS residual distribution in the last ten years.

VI. BOUNDING THE RESIDUALS

Two categories of paired-bound are computed in this section. Group paired-bound continues the latitude-wise grouping criteria established in Section.IV.1. The paired-bounds bound the residual distribution group by group, and as a result, could apply less stringent paired-bound depending on the locations. Overall paired-bound essentially combine all stations into a single group for it to be bounded. The overall paired-bound could provide general boundness to all stations but are a more conservative bound to the tropospheric residual uncertainties. In this section, we evaluate residuals of UNB3. Bounding parameters for GPT series are referred to the Appendix.

1. Group Paired-Bound

a) Minimal Bias

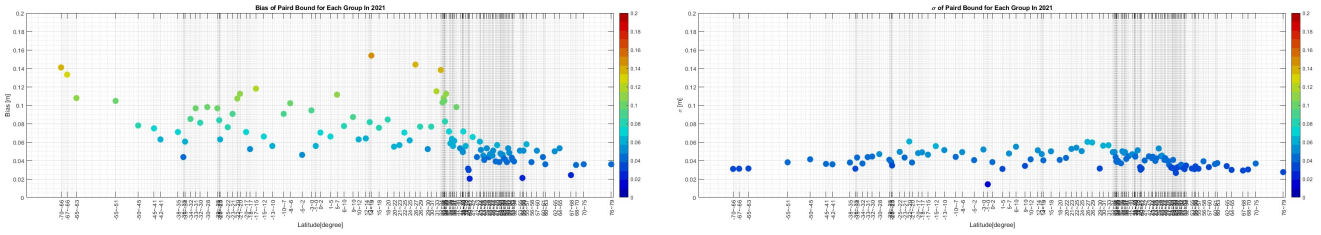

(a) Bias of Group Paired-Bound

(b) Std of Group Paired-Bound

Figure 9: Group Minimal Bias Gaussian Paired-Bound in 2021.

Fig.9 represent the Gaussian paired-bound for each latitude-wise group. Fig.9a is the minimal bias of the paired-bound computed from the Ad-hoc algorithm. The minimal bias is dependent on median value but may also affected by the tail or head of the residual distribution. Overall, the bias is distributed similar to Fig.3, with lower bias in latitude $30^\circ \sim 50^\circ$ and have the same increasing pattern when lower than -40°. The median essentially determines how wide the paired-bound must be in order for it to be bounded. If the residual is Gaussian distribution, the median value of the residual is the minimal bias, any paired-bound with bias lower than that would failed to bound the distribution. Fig.9b is the standard deviation of the paired-bound. It follows the symmetric pattern of Max/Min residuals of UNB3, with most of them below 6 cm.

b) Constant Bias and Constant Standard Deviation

Constant bias selects a fixed bias value, then searching the minimal standard deviation that bounds the residual distribution. This is similar to the minimal bias process except the bias value is specified in stead of determined from search process. Constant standard deviation is the opposite of constant bias, which chooses standard deviation first, then minimizing the corresponding bias value. Minimizing bias and standard deviation brings up the reciprocal relation of these two parameters. The higher the bias, the smaller the standard deviation, and vice versa. The extreme case in our application is when bias is greater than 28 cm, the bias itself can bound the entire residual distribution such that the corresponding standard deviation can be zero, which is equivalent to assuming all tropospheric delay predictions have 28 cm of error. On the other hand, enlarging standard deviation would not reduce bias to lower than median owing to Gaussian paired-bound is a straight line on QQ-plot. This is the trade-off between bias and standard deviation for paired-bound, and the relative importance of bias and uncertainties depend on the purpose of application.

2. Overall Paired-Bound

The issue with Group paired-bound is the validity of bounds depends on the latitude, the bounding parameters bias and standard deviation need to change according to the user location. While it offers tighter bounds to the user, it requires extra complexity and storage requirement to SBAS. Overall paired-bound simplify the latitude-wise sorting criteria by finding one bound that covers the entire residual distribution for all IGS stations regardless of their location. This overall paired-bound inevitably introduce conservatism to the bounding parameters comparing to group paired-bound, but allows simpler bounding logic for the user.

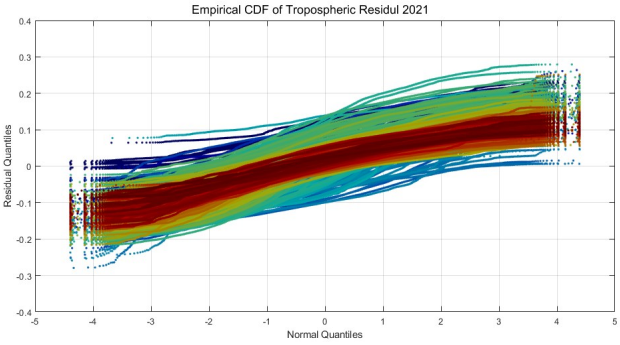

Figure 10: Overall residual paired-bound in 2021.

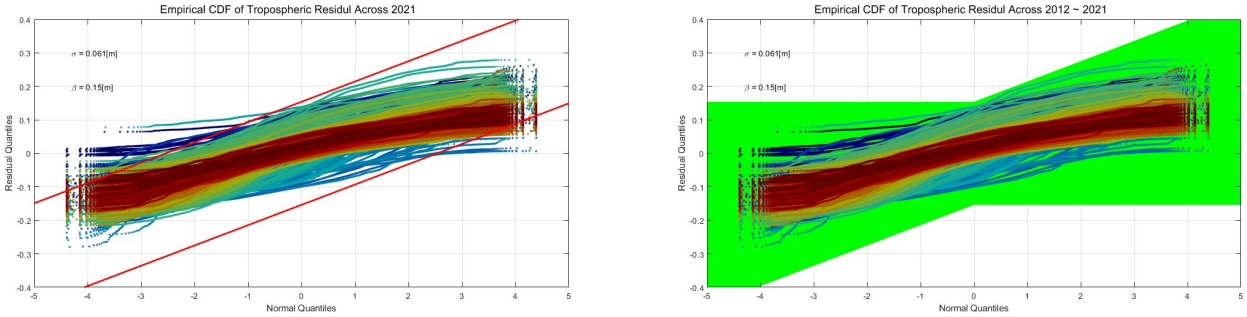

(a) Overall Paired-Bound

(b) Overall Paired-Bound - Valid Region

Figure 11: Overall Paired-Bound in 2021.

Fig.10 is the residual distribution in 2021. Fig.11a shows the overall minimal bias paired-bound for the whole residual distribution as two red lines. The bound is produced from minimal bias algorithm, and the resulting bias is 0.1538 m and the standard deviation is 0.0606 m. The red straight lines construct the paired-bound region. We can see there are some part of the residuals outside of the bounding region, but since we chose the larger bias and larger standard deviation for each residual distribution, the seemly unbounded residuals are in fact properly bounded by the Gaussian paired-bound in VPL. The green region in Fig.11b is the valid region for the paired-bound parameters and all residual are inside.

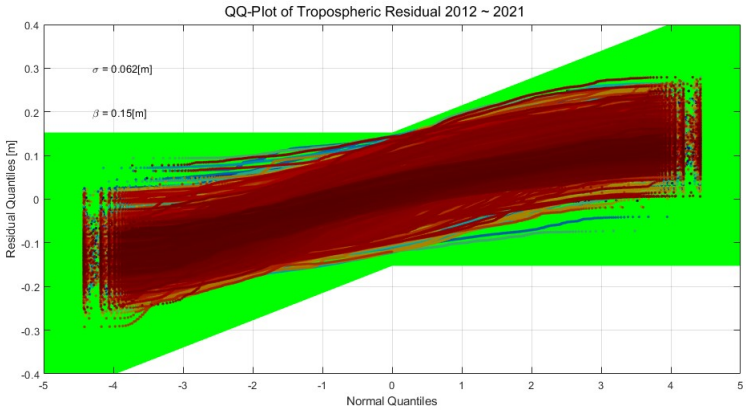

Figure 12: Overall residual in 2012∼2021.

Fig.12 is the entire residual distribution of all IGS stations in 2012 $\sim$ 2021 and its paired-bound region. The bias is 0.1526 m and the corresponding standard deviation is 0.0624 m. The bias is the same as the overall bound in 2021 implies the station in

2021 has the largest minimal bias among all other stations, and the standard deviation is slightly higher. These two parameters bound the residuals for all IGS stations from 2012 to 2021, and could be the choice for alternate SBAS VPL equation introduced in Section.VII.

VII. ALTERNATE SBAS VPL

1. Current SBAS VPL

Current SBAS VPL adopt the scheme of real-time protection level, which contains:

Variance on satellite i:

$$\sigma_i^2 = \sigma_{i,flt}^2 + \sigma_{i,air}^2 + \sigma_{i,tropo}^2 + \sigma_{i,UIRE}^2 \tag{5}$$

where $\sigma_{i,flt}^2$ is fast and long-term correction correction error, $\sigma_{i,air}^2$ is the airborne error including multipath error, $\sigma_{i,tropo}^2$ is tropospheric error and $\sigma_{i,UIRE}^2$ is User Ionospheric Range Error. In particular, the tropospheric errors are treated as independent from satellite to satellite.

Geometric Matrix $\boldsymbol{G}$:

$$\overrightarrow{y} = \boldsymbol{G} \cdot \overrightarrow{x} \tag{6}$$

where $\overrightarrow{y}$ is a vector of pseudorange measurement from the line-of-sight satellites in view to the user. $\overrightarrow{x}$ is the position and clock bias estimation of the user. $\boldsymbol{G}$ is the geometric matrix that map position into line-of-sight domain, and is composed of normalized line-of-sight vector.

Weighting Matrix $\boldsymbol{W}$:

$$\boldsymbol{W} = \begin{bmatrix} \sigma_1^2 & 0 & \dots & 0 \\ 0 & \sigma_2^2 & \dots & 0 \\ \vdots & \ddots & \ddots & \vdots \\ 0 & 0 & \dots & \sigma_n^2 \end{bmatrix}^{-1} \tag{7}$$

Position Covariance Matrix $\boldsymbol{d}$:

$$\boldsymbol{d} = \left(\boldsymbol{G}^T \cdot \boldsymbol{W} \cdot \boldsymbol{G}\right)^{-1} \tag{8}$$

Projection Matrix $\boldsymbol{S}$:

$$\boldsymbol{S} = \left(\boldsymbol{G}^T \cdot \boldsymbol{W} \cdot \boldsymbol{G}\right)^{-1} \cdot \boldsymbol{G}^T \cdot \boldsymbol{W} \tag{9}$$

where the projection matrix, $\boldsymbol{S}$, projects the pseudorange measurement into position domain. Note that it is also the optimal solution to the weighted least-square problem.

VPL:

$$VPL = K_V \cdot d_U \tag{10}$$

where K_V is a constant with value of 5.33, corresponding to inverse standard normal distribution with integrity budget allocated to vertical direction, and is standard for VAL below 10 m. d_U is the position variance in vertical direction, or the Up in East-North-Up (ENU) coordinate system. We see the current VPL equation depends on variance of the vertical position, and therefore depends on the nominal error model we used in the calculation of σ_i^2.

MOPS mappung function:

$$m(EL[i]) = \frac{1.001}{\sqrt{0.002001 + sin^2(EL[i])}} \tag{11}$$

$$\overrightarrow{m} = \begin{bmatrix} m(EL[1]) \\ m(EL[2]) \\ \vdots \\ m(EL[n]) \end{bmatrix} \tag{12}$$

where $EL[i]$ is the elevation angle of i^{th} satellite, and n is the total number of satellites in view for the receiver.

To ensure VPL is robust and fault tolerant in any valid condition for the uncertainties of tropospheric delay in current nominal error model, we randomly generate line-of-sight uni-vector for geometric matrix, $\boldsymbol{G}$, and randomly select elevation angles for line-of-sight measurement and tropospheric delay, then projection matrix, $\boldsymbol{S}$, project maximal nominal tropospheric delay model uncertainties, 28cm, along with mapping function, into position domain. The resulting vertical position error is compared with the corresponding VPL.

a) Uniform Random Simulation - Current SBAS VPL

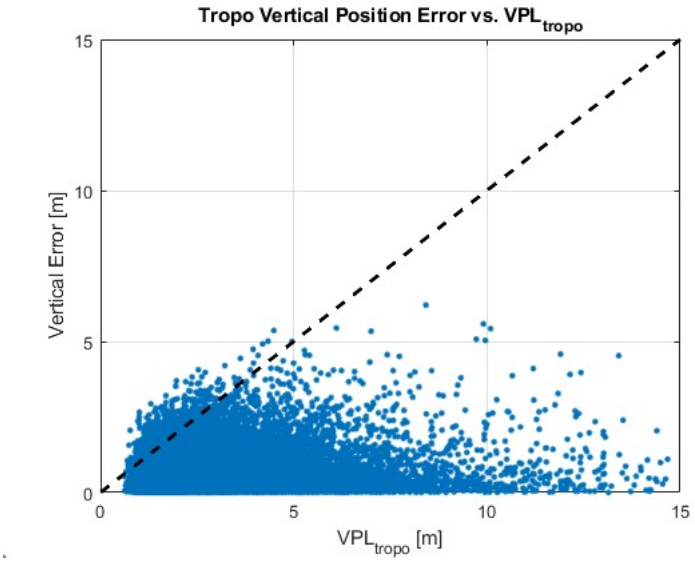

Figure 13: SBAS Tropospheric Error vs. VPL

Fig.13 is the possible positioning error versus the VPL. The positioning error is computed from Eq.(9) with 28cm zenith total delay error in measurement, and VPL is from Eq.(10). This simulation assume 12 satellites in-view for one constellation and randomly generate 50000 geometric matrices. A diagonal dash-line is drawn to facilitate the determination of whether the vertical error exceed the VPL. We can see there is a small portion of vertical errors are above the diagonal line, indicating the possible vertical errors might be underestimated due to the simplification that tropospheric errors are uncorrelated across satellites.

One thing to notice is it does not mean the tropospheric correlation error resulting in position error unbounded, it merely shows that there exist combinations of geometric matrices and elevation angles that might result in higher vertical error than the VPL. The simulation takes the most extreme case of tropospheric delay error as the sole factor to the estimation of the VPL, ignoring contributions of duel-frequency correction error, air error etc. In SBAS, since tropospheric delay error is not the only error we consider in position estimation, there is no immediate issue to the integrity of position solution.

2. Alternate SBAS VPL

Acknowledging that current VPL might underestimate the possible effect of nominal tropospheric to position error, we suggest a modified VPL equation that includes the correlation from one satellite to another and the uncertainties of tropospheric residual distribution into VPL calculation.

To support correlation and biased tropospheric error, we separate covariance contribution into non-tropospheric and tropospheric.

Non-tropospheric variance:

$$\sigma_{i,nt}^2 = \sigma_{i,flt}^2 + \sigma_{i,air}^2 + \sigma_{i,UIRE}^2 \tag{13}$$

Non-tropospheric position variance:

$$d_{nt,U}^2 = \sum_{i}^{n} s_{3,i}^2 \cdot \sigma_{i,nt}^2 \tag{14}$$

Scaling for tropospheric to position error:

$$f_{t,U} = \| \sum_{i}^{n} s_{3,i} \cdot m(EL[i]) \| \tag{15}$$

New VPL:

$$VPL_{new} = K_V \cdot \sqrt{d_{nt,U}^2 + \sigma_{TVE}^2 \cdot f_{t,U}^2} + \beta_{TVE} \cdot f_{t,U} \tag{16}$$

where $d_{nt,U}^2$ is the position variance without tropospheric effect, $f_{t,U}$ is the mapping from tropospheric error to position error domain. σ_{TVE}^2 and β_{TVE} are the variance and bias of zenith tropospheric residual.

a) Uniform Random Simulation - Corrected SBAS VPL

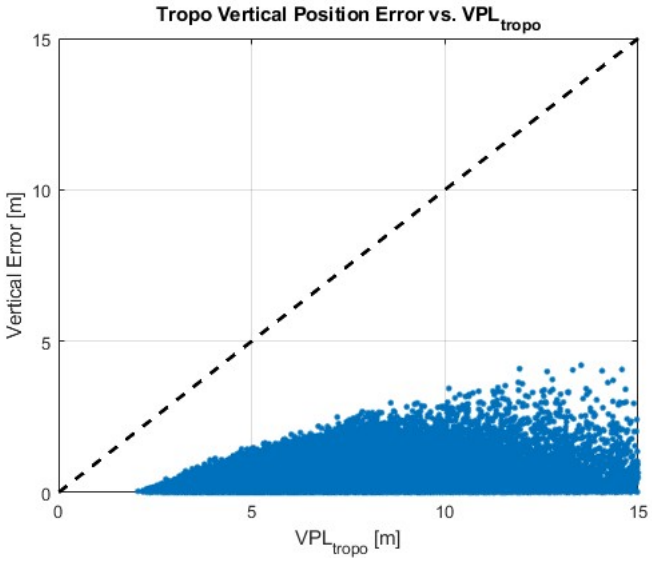

Figure 14: SBAS Tropospheric Error vs. Corrected VPL

Fig.14 is the vertical position error versus the corrected VPL. The only difference between Fig.13 and Fig.14 is the VPL equation. The new VPL equation bound all the possible combination of geometric matrices and elevation angle by incorporating the satellite correlations and Gaussian tropospheric residual bound, where the paired-bound parameters are the overall paired-bound of UNB3. σ_{TVE} and β_{TVE} used in the simulation are the overall bound we obtained from ten years of data in Sec.VI. With the new VPL equation, all possible position error are below the corresponding VPL.

The modification to the VPL equation does not require anything new to the SBAS except σ_{TVE} and β_{TVE}, which can be two constants added to the system like we did in the simulation, or a table of values based on locations.

3. Sigma-Bias Value for Alternate VPL Equation

Other sigma-bias values are also possible to be used in the alternate VPL equation. Appendix VIII.2 shows the relation of sigma and bias values for UNB3 model in the ten-year IGS data. There is a reciprocal relation between sigma and bias values, so the minimal bias corresponds to maximum sigma, and vice versa.

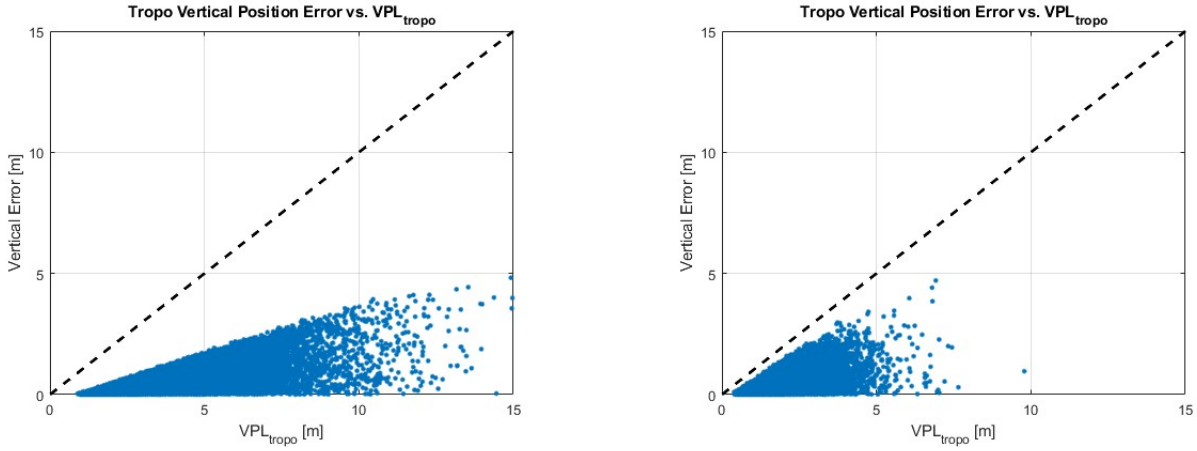

(a) SBAS Tropospheric Error vs. Corrected VPL

(b) SBAS Tropospheric Error vs. Corrected VPL

Figure 15: SBAS Tropospheric Error vs. Corrected VPL without Non-tropo errors

Fig.15 represent different sigma-bias value can have different vertical error versus alternate VPL when non-tropospheric errors are not included. Fig.15a has $\sigma = 0.12$ m and $\beta = 0$ m. Fig.15b has $\sigma = 0$ m and $\beta = 0.28$ m. Both sigma-bias values are capable of bounding the tropospheric error, and Fig.15b has VPL closer to vertical error, so the VPLs are smaller and still can bound the error. As a result, $\sigma = 0$ m and $\beta = 0.28$ m is a better sigma-bias value when tropospheric error is the sole factor to the calculation of alternate VPL.

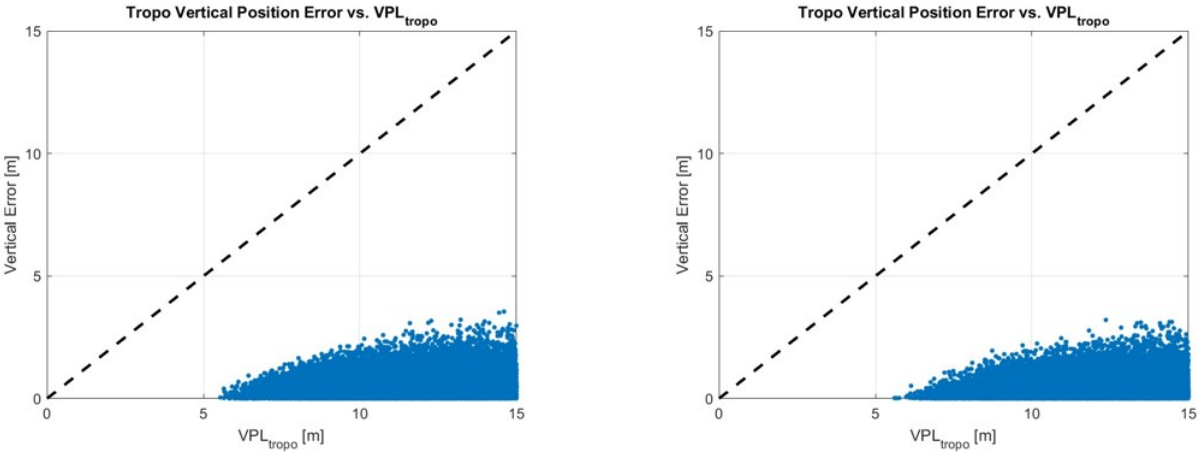

(a) SBAS Tropospheric Error vs. Corrected VPL

(b) SBAS Tropospheric Error vs. Corrected VPL

Figure 16: SBAS Tropospheric Error vs. Corrected VPL with Non-tropo errors

Fig.16 show the vertical error versus VPL when non-tropospheric errors are included in the calculation of VPL, so $d_{nt,U} \neq 0$. Fig.16a has $\sigma = 0.12$ m and $\beta = 0$ m. Fig.16b has $\sigma = 0$ m and $\beta = 0.28$ m. We can see with the non-tropospheric error included into the calculation of the alternate VPL, Fig.16a has smaller VPL than Fig.16b. Contrary to the result without non-tropospheric error. The reason for this is the non-tropospheric error, $d_{nt,U}$, is typically larger than tropospheric error, σ_{TVE}, so after the root-mean-square process in Eq.16, the contribution of tropospheric error to VPL is smaller. For $\sigma = 0$ m and $\beta = 0.28$, the contribution of tropospheric error to VPL is a linear addition so the resulting VPL is larger. Therefore, with non-tropospheric error included into the calculation of alternate VPL, larger sigma value provides better result.

VIII. CONCLUSION

We examined the tropospheric delay data of all IGS stations from 2012 to 2021. The tropospheric prediction from three models, UNB3, GPT2W and GPT3 are evaluated and compared with data from IGS stations to form the residual distribution at each station in every year. Some IGS data were excluded from the computation of residual due to anomalous value after cross-validating against the weather record and JPL data. An Ad-hoc algorithm was developed to compute Gaussian paired-bound to bound the distribution of residual. There are thee types of bounds, minimal bias, constant bias and constant standard deviation. Minimal bias obtained the lowest bias for paired-bound and automate the whole process. Constant bias and constant standard deviation are relaxations to the minimal bias and need manually assigning one of paired-bound parameters. Residuals from 2012 to 2021 of UNB3, GPT2W and GPT3 are all successfully bounded with the paired-bound generated by Ad-hoc algorithm.

A simulation result shows that current VPL equation might significantly underestimate the nominal tropospheric to position error when VAL is below 10 m. Therefore, we proposed a modification to current SBAS VPL equation such that the tropospheric correlations of satellites can be accounted into the calculation of VPL. The paired-bound parameters computed are also integrated into the VPL equation. Another simulation result shows the alternate VPL equation with the paired-bound parameters computed from IGS data gives more conservative VPL for VAL below 10 m. Finally, different sigma-bias values are possible for the alternate VPL equation depending on the non-tropospheric error sources. The new VPL equation can be easily adapted to current SBAS system with paired-bound parameters suggested in this paper.

APPENDIX

1. Overall Minimum Bias Paired-Bound

a) UNB3

Bias	0.1526 [m]
Standard Deviation	0.0624 [m]

b) GPT2W

Bias	0.1483 [m]
Standard Deviation	0.0732 [m]

c) GPT3

Bias	0.1483 [m]
Standard Deviation	0.0732 [m]

2. Overall Sigma-Bias relation:UNB3

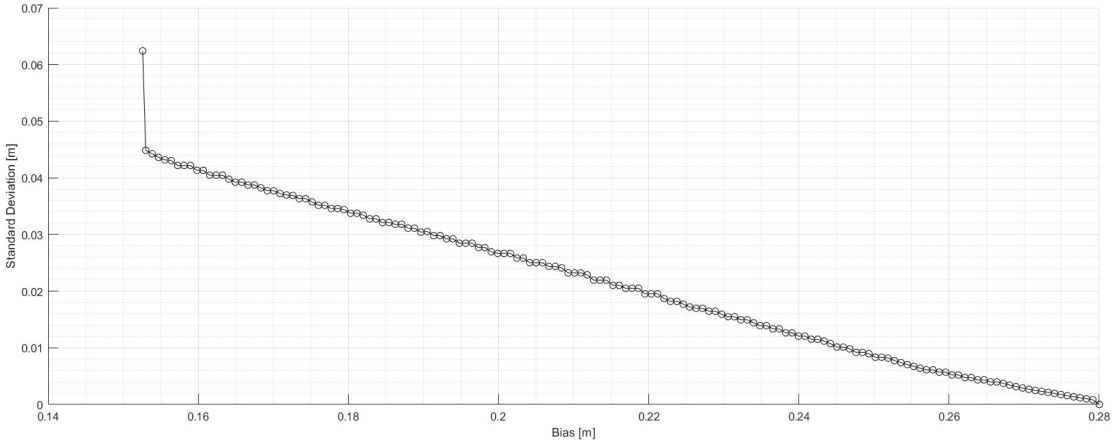

Figure 17: σ-β relation.

ACKNOWLEDGEMENTS

We gratefully acknowledge the support of the FAA Satellite Navigation Team for funding this work under Memorandum of Agreement #: 693KA8-22-N-00015. We also thank Dr. Attila Komjathy and Dr. Angelyn Moore of JPL and Dr. Sharyl Byram of USNO for providing useful suggestion on evaluating tropospheric ZPD.

REFERENCES

Bertiger, W., Bar-Sever, Y., Dorsey, A., Haines, B., Harvey, N., Hemberger, D., Heflin, M., Lu, W., Miller, M., Moore, A. W., et al. (2020). Gipsyx/rtgx, a new tool set for space geodetic operations and research. *Advances in space research*, 66(3):469–489.

Black, H. and Eisner, A. (1984). Correcting satellite doppler data for tropospheric effects. *Journal of Geophysical Research: Atmospheres*, 89(D2):2616–2626.

Blanch, J., Walter, T., and Enge, P. (2018). Gaussian bounds of sample distributions for integrity analysis. *IEEE Transactions on Aerospace and Electronic Systems*, 55(4):1806–1815.

Böhm, J., Möller, G., Schindelegger, M., Pain, G., and Weber, R. (2015). Development of an improved empirical model for slant delays in the troposphere (gpt2w). *GPS solutions*, 19(3):433–441.

Collins, J. P. and Langley, R. B. (1997). *A tropospheric delay model for the user of the wide area augmentation system*, volume 20. Department of Geodesy and Geomatics Engineering, University of New Brunswick . . . .

Davis, J., Herring, T., Shapiro, I., Rogers, A., and Elgered, G. (1985). Geodesy by radio interferometry: Effects of atmospheric modeling errors on estimates of baseline length. *Radio science*, 20(6):1593–1607.

DeCleene, B. (2000). Defining pseudorange integrity-overbounding. In *Proceedings of the 13th International Technical Meeting of the Satellite Division of The Institute of Navigation (ION GPS 2000)*, pages 1916–1924.

EUROCAE (2023.). Ed-259a: minimum operational performance specification for galileo/global positioning system/satellite-based augmentation system airborne equipment, v0.16 (draft).

Gallon, E., Joerger, M., and Pervan, B. (2021). Robust modeling of gnss tropospheric delay dynamics. *IEEE Transactions on Aerospace and Electronic Systems*, 57(5):2992–3003.

IGS, M. (2022). International gnss service.

Juan Blanch, Yu-Fang Lai, T. W. (2023). Evaluation of tropospheric and mixed single - dual frequency error models in advanced raim. *Proceedings of ION ITM*.

Landskron, D. and Böhm, J. (2018). Vmf3/gpt3: refined discrete and empirical troposphere mapping functions. *Journal of Geodesy*, 92(4):349–360.

McGraw, G. A. (2012). Tropospheric error modeling for high integrity airborne gnss navigation. In *Proceedings of the 2012 IEEE/ION Position, Location and Navigation Symposium*, pages 158–166. IEEE.

Rife, J., Pullen, S., Enge, P., and Pervan, B. (2006). Paired overbounding for nonideal laas and waas error distributions. *IEEE Transactions on Aerospace and Electronic Systems*, 42(4):1386–1395.

RTCA (2006.). Minimum performance operational standards (mops) for global positioning system/satellite-based augmentation airborne equipment. rtca document do-229d.

Vollmer, B. E., Ostrenga, D., Savtchenko, A., Johnson, J., Wei, J., Teng, W., and Gerasimov, I. (2011). Making earth science data records for use in research environments (measures) projects data and services at the ges disc. Technical report.